



**HAL**  
open science

## **Planar polarity of multiciliated ependymal cells involves the anterior migration of basal bodies regulated by non-muscle myosin II**

Yuki Hirota, Alice Meunier, Shihhui Huang, Togo Shimosawa, Osamu Yamada, Yasuyuki S Kida, Masashi Inoue, Tsubasa Ito, Hiroko Kato, Masanori Sakaguchi, et al.

### ► To cite this version:

Yuki Hirota, Alice Meunier, Shihhui Huang, Togo Shimosawa, Osamu Yamada, et al.. Planar polarity of multiciliated ependymal cells involves the anterior migration of basal bodies regulated by non-muscle myosin II. *Development (Cambridge, England)*, 2010, 137 (18), pp.3037 - 3046. 10.1242/dev.050120 . hal-04477363

**HAL Id: hal-04477363**

**<https://hal.science/hal-04477363>**

Submitted on 26 Feb 2024

**HAL** is a multi-disciplinary open access archive for the deposit and dissemination of scientific research documents, whether they are published or not. The documents may come from teaching and research institutions in France or abroad, or from public or private research centers.

L'archive ouverte pluridisciplinaire **HAL**, est destinée au dépôt et à la diffusion de documents scientifiques de niveau recherche, publiés ou non, émanant des établissements d'enseignement et de recherche français ou étrangers, des laboratoires publics ou privés.

Development 137, 0000-0000 (2010) doi:10.1242/dev.050120  
 © 2010. Published by The Company of Biologists Ltd

# Planar polarity of multiciliated ependymal cells involves the anterior migration of basal bodies regulated by non-muscle myosin II

Yuki Hirota<sup>1</sup>, Alice Meunier<sup>2</sup>, Shihhui Huang<sup>1</sup>, Togo Shimosawa<sup>3</sup>, Osamu Yamada<sup>4</sup>, Yasuyuki S. Kida<sup>5</sup>, Masashi Inoue<sup>1</sup>, Tsubasa Ito<sup>1</sup>, Hiroko Kato<sup>1</sup>, Masanori Sakaguchi<sup>4</sup>, Takehiko Sunabori<sup>4</sup>, Masa-aki Nakaya<sup>6</sup>, Shigenori Nonaka<sup>7</sup>, Toshihiko Ogura<sup>5</sup>, Hideo Higuchi<sup>3</sup>, Hideyuki Okano<sup>4</sup>, Nathalie Spassky<sup>2</sup> and Kazunobu Sawamoto<sup>1,\*</sup>

## SUMMARY

Motile cilia generate constant fluid flow over epithelial tissue, and thereby influence diverse physiological processes. Such functions of ciliated cells depend on the planar polarity of the cilia and on their basal bodies being oriented in the downstream direction of fluid flow. Recently, another type of basal body planar polarity, characterized by the anterior localization of the basal bodies in individual cells, was reported in the multiciliated ependymal cells that line the surface of brain ventricles. However, little is known about the cellular and molecular mechanisms by which this polarity is established. Here, we report in mice that basal bodies move in the apical cell membrane during differentiation to accumulate in the anterior region of ependymal cells. The planar cell polarity signaling pathway influences basal body orientation, but not their anterior migration, in the neonatal brain. Moreover, we show by pharmacological and genetic studies that non-muscle myosin II is a key regulator of this distribution of basal bodies. This study demonstrates that the orientation and distribution of basal bodies occur by distinct mechanisms.

**KEY WORDS:** Planar cell polarity, Ependymal cell, Cilia, Dvl2, Non-muscle myosin II, Mouse

## INTRODUCTION

Motile cilia are membrane protrusions that move rapidly to generate fluid flow or to move materials present in the extracellular space. To generate directional fluid flow over the surface of a tissue, ciliary beating must be coordinated in the same direction. Recent studies have shown that the planar cell polarity (PCP) pathway, a downstream branch of Wnt signaling, plays important roles in directing the ciliary beating of multiciliated cells in *Xenopus* larval skin and mouse ependymal cells (Ganner et al., 2009; Guirao et al., 2010; Mitchell et al., 2007; Mitchell et al., 2009; Park et al., 2008; Tissir et al., 2010). In addition, fluid flow-mediated mechanisms and functional ciliary axonemes are involved in establishing the planar polarity of ciliary orientation (Guirao et al., 2010; Mitchell et al., 2007). Recently, a novel ependymal cell PCP, characterized by the anterior positioning of basal bodies, was reported and termed ‘translational’ polarity (Mirzadeh et al., 2010). Another planar polarity indicated by the direction of the basal foot was termed ‘rotational’ by the same group. Recent studies have

revealed the cellular and molecular mechanisms underlying the rotational polarity of ependymal cells (Guirao et al., 2010; Mirzadeh et al., 2010; Tissir et al., 2010). By contrast, the mechanisms of translational polarity formation during postnatal ependymal development have not been elucidated.

Recently, non-muscle myosin II (NMII) was shown to play important roles in PCP formation in invertebrates and vertebrates (Bertet et al., 2004; Skoglund et al., 2008; Yamamoto et al., 2009). NMII is a hexameric protein consisting of two heavy chains (non-muscle myosin heavy chains, NMHCs) that form a dimer, a pair of regulatory light chains (RLCs), and a pair of essential light chains. The disruption of NMII causes hydrocephalus (Ma et al., 2007), suggesting that NMII is involved in the maturation of ependymal cilia. However, the exact role of NMII in the differentiation of ependymal cells remains unknown.

We show here that translational polarity is established by the anterior migration of basal bodies in the apical membrane during the differentiation of ependymal cells. We also show that NMII is a key regulator of this process.

## MATERIALS AND METHODS

### Animals

Wild-type ICR mice were purchased from SLC. Centrin 2::GFP (Cent2GFP) transgenic mice were described previously (Higginbotham et al., 2004). All animal experimental procedures complied with national regulations and guidelines, were reviewed by the Institutional Laboratory Animal Care and Use Committee, and were approved by the President of Nagoya City University.

### Histological analysis

Immunostaining of whole-mount lateral ventricular walls was performed as described previously (Hirota et al., 2007). The following antibodies were used: rabbit anti-pericentrin (Pcnt); (1:500; Covance, PRB-432C); goat

<sup>1</sup>Department of Developmental and Regenerative Biology, Nagoya City University Graduate School of Medical Sciences, Nagoya 467-8601, Japan. <sup>2</sup>Institut de Biologie de l’Ecole Normale Supérieure (IBENS), Institut National de la Santé et de la Recherche Médicale U1024, Centre National de la Recherche Scientifique UMR8197, 75005 Paris, France. <sup>3</sup>Department of Physics, Graduate School of Science, University of Tokyo, Tokyo 113-0033, Japan. <sup>4</sup>Department of Physiology, Keio University School of Medicine, Tokyo 160-8582, Japan. <sup>5</sup>Department of Developmental Neurobiology, Institute of Development, Aging and Cancer, Tohoku University, Sendai 980-8575, Japan. <sup>6</sup>Department of Histology and Embryology, Kanazawa University Graduate School of Medical Science, Kanazawa 920-8640, Japan. <sup>7</sup>NIBB Laboratory for Spatiotemporal Regulation, NIBB, Okazaki 444-8585, Japan.

\* Author for correspondence (sawamoto@med.nagoya-cu.ac.jp)

anti- $\gamma$ -tubulin (1:100; Santa Cruz, sc7396); mouse CTR453 (1:10) (Bailly et al., 1989); mouse anti- $\beta$ -catenin (1:200; BD 610154); chick anti-GFP (1:500; Aves, 2-P004-07D); rat anti-GFP (1:500; Nacalai, GF090R); rabbit anti-GFP (1:100; MBL); rabbit anti-Dvl2 (1:300; Santa Cruz, sc-13974); mouse anti-acetylated tubulin (1:1000; Sigma, T6793); rabbit anti-Myh9 (1:300; Covance, PRB-440P); rabbit anti-Myh10 (1:300; Covance, PRB-445P); rabbit anti-Myh14 (1:300; Covance, PRB-444P); rabbit pMLC2 (My19) (1:200; Cell Signaling, 3674); rat R4109 (1:2) (Hagiwara et al., 2000); mouse anti-ZO1 (1:300; Zymed, 33-9100); and species-specific secondary antibodies (Invitrogen or Jackson ImmunoResearch). Confocal images were obtained using LSM5-Pascal and LSM710 (Zeiss) microscopes. Scanning electron microscopy analyses were performed as described previously (Sawamoto et al., 2006) using an S-5000 (Hitachi) electron microscope. Immunotransmission electron microscopy (TEM) analyses using rabbit anti-GFP antibody were performed as described previously (Yamashita et al., 2006) using a JEM-1200EX (JEOL) electron microscope.

### Ependymal cell culture

The detailed protocol for the primary culture of ependymal cells and the device used to create the artificial fluid flow have been described previously (Guirao et al., 2010). For transfections, ependymal cells in 24-well plates were transfected with Lipofectamine (Invitrogen) and 500 ng of plasmid DNA per well. For the visualization of beating cilia, ependymal cells were labeled using the PKH26 Fluorescent Cell Linker Kit (Sigma) or FluoSpheres carboxylate-modified microspheres (Invitrogen, F8801). The movement of the beads was recorded using a BX51 microscope (Olympus).

### Quantification of the rotational orientation of cilia

To quantify the direction of ciliary beating on cultured ependymal cells, the movement of beads attached to the cilia was traced (lines in Fig. 4H–J, 11–25 cilia in each cell), and the angle of the beating direction of each cilium from the mean direction was determined for each cell. Using Oriana 2.0 (Kovach Computing Services) circular statistics software, the circular standard deviation (CSD) in each cell was calculated as described previously (Guirao et al., 2010; Mitchell et al., 2007; Park et al., 2008) and compared using a two-tailed, unpaired Student's *t*-test. The basal body orientation in the ventricular walls was analyzed as described previously (Guirao et al., 2010) with modifications. Briefly, 5–11 basal feet in each ependymal cell from 2–5 ultrathin sections were analyzed. A vector was drawn from the center of the basal body to the protrusion of the basal foot, and the angle of this vector from the anterior direction (defined as 0°) was determined using ImageJ software. These data were analyzed using Oriana 2.0 software, and the output was expressed on a circular plot as a vector with an angle that denotes the mean ciliary direction and a length that denotes the complement of the circular variance of these cilia around the mean. The circular distributions of the basal feet within each cell were compared with a random distribution using Rayleigh's test.

### Quantification of basal body distribution

The positions of the centroids of the ciliated region (shown by a basal body marker) and the whole cell (shown by a cell border marker) were calculated using ImageJ software. Ependymal cells with the entire cell border within the focal plane were selected and analyzed. Ependymal cells in which the centroid of the ciliated region was within 90° of the anterior (rostral) direction relative to the centroid of the whole cell were classified as having an 'anterior' localization of the basal body. For the transfection of dominant-negative forms of Dvl2 and the knockdown of NMII, 5–12 cells per animal were analyzed. For the inhibitor experiments, 15–53 cells per animal were analyzed.

### Time-lapse imaging of basal bodies

Lateral walls from P5–8 Cent2GFP mice were embedded in 80% Matrigel (BD Biosciences) diluted in L-15 on glass-bottomed dishes. Time-lapse recordings were performed as described previously (Hirota et al., 2007), using a 63 $\times$  oil-immersion objective lens.

### High-speed live imaging of ciliary beating

Brain slices (200  $\mu$ m thick) from P4–6 or P14–19 Cent2GFP mice were labeled using the PKH26 Fluorescent Cell Linker Kit (Sigma). The optical system for observing the fluorescence consisted of an epifluorescence microscope (IX-71, Olympus) equipped with a 60 $\times$  water-immersion objective (UPLSAPO60XW, 1.20 NA; Olympus), a Nipkow disk-type confocal unit (CSU22, Yokogawa) and an electron multiplying CCD camera (iXon860BV, Andor Technology). For the inhibitor experiments, we used an inverted Zeiss LSM5 LIVE scanner. The images of beating cilia were recorded at 917 or 542 frames per second at room temperature (24–26°C).

### DNA constructs and lentivirus expression vector

The mouse Dvl2 $\Delta$ PDZ construct was described previously (Habas et al., 2001). The C-terminus of Dvl2 (Dvl2-C), spanning amino acids 508–736, was amplified by PCR. Plasmids encoding GFP fusion proteins (Dvl2 $\Delta$ PDZ-GFP, Dvl2-C-GFP) were constructed using pEGFP-N1 (Clontech), which was also used as the control vector. Dvl2 $\Delta$ PDZ-GFP was subcloned into self-inactivating lentivirus vector CSII-EF-MCS (provided by Dr H. Miyoshi, Riken Tsukuba BioResource Center) (Miyoshi et al., 1998) to produce CSII-EF-Dvl2 $\Delta$ PDZ-GFP. Lentiviruses were produced as described previously (Kojima et al., 2010). For the knockdown experiments, the targeting sequences of *Myh9*, *Myh10* and *Myh14* (miR RNAi Select, Invitrogen) and *lacZ* (control) were cloned into a modified Block-iT Pol II miR RNAi expression vector (Invitrogen). DNA cassettes containing DsRed-Express (Clontech) and the targeting sequence were cloned into pCAGGS vectors (Niwa et al., 1991) using the Gateway system (Invitrogen).

### Injection and electroporation

Injection of lentivirus was performed as described previously (Kojima et al., 2010). For the inhibitor experiments, 1.5  $\mu$ l of 5 mM (high dose) or 2.5 mM (low dose) inhibitor or vehicle was stereotaxically injected into the lateral ventricle of P4–5 mice [relative to lambdoid suture of the skull, anterior, lateral, depth (mm): 2.0, 1.0, 1.8]. The following inhibitors were used: blebbistatin (dissolved in 50% methanol in PBS, Research Chemicals); ML-9 (dissolved in 50% methanol in PBS, Calbiochem); Y27632 (dissolved in PBS, Calbiochem); and SP600125 (dissolved in 25% DMSO in PBS, Calbiochem). Electroporation of P1 mice was performed as described previously (Boutin et al., 2008).

### Statistical analyses

All data are expressed as the mean  $\pm$  s.e.m. Differences between means were determined by unpaired two-tailed Student's *t*-test. For the inhibitor experiments, the data were analyzed by one-way ANOVA followed by Tukey's multiple comparison test. For the circular analysis, we used the Oriana 2.0 program. *P* < 0.05 was considered significant.

## RESULTS

### Basal bodies of ependymal cilia gradually translocate to the anterior region of ependymal cells during differentiation

To examine how translational polarity is established during the differentiation of ependymal cells, whole-mount lateral ventricular walls were prepared from mice of different ages. The anteroposterior (A–P) orientation of tissues was determined by the asymmetrical shape of the whole-mount ventricular walls (Fig. 1). They were then immunostained for Pcnt and ZO1 (Tjp1 – Mouse Genome Informatics), markers for basal bodies and tight junctions, respectively. To standardize our analysis, we used only the dorsal part of the medial lateral ventricle (Fig. 1). In the early stages of ciliogenesis, the basal bodies were broadly distributed in the apical membrane of immature ependymal cells (Fig. 1A). The basal bodies gradually became asymmetrically localized within the apical membrane, accumulating at the anterior region of each ependymal cell (i.e. downstream in terms of the ciliary beating direction) (Fig. 1B). By P9, the basal bodies had formed a dense accumulation in the anterior region of most ependymal cells (Fig. 1C). In the adult,

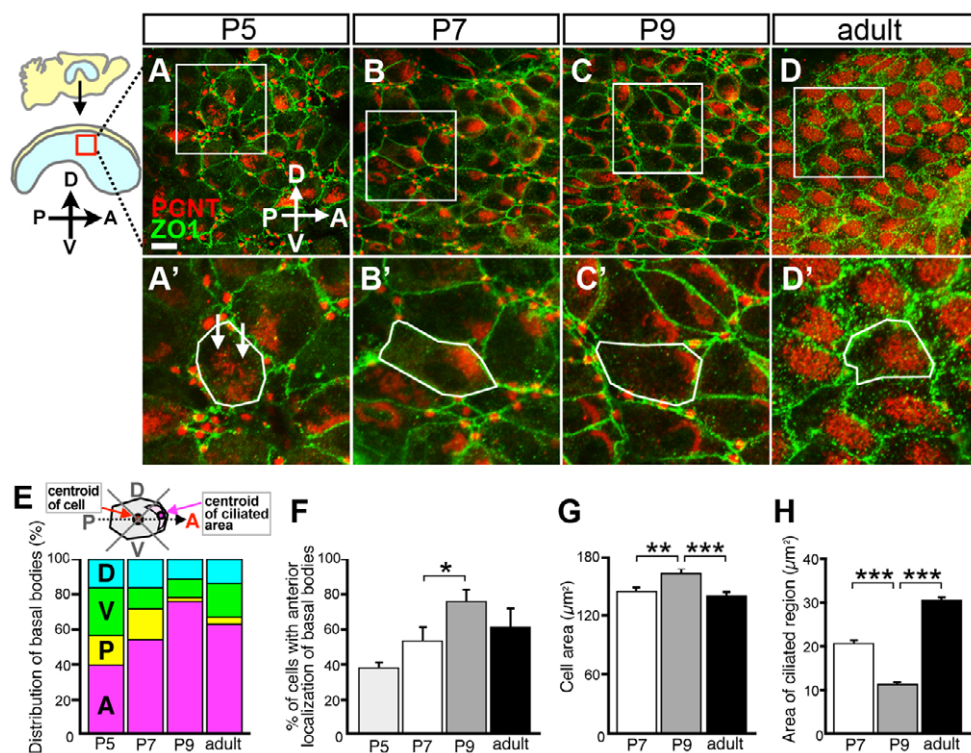


**Fig. 1. Alteration of basal body distribution during the differentiation of ependymal cells.** (A–D') To the left is a schematic showing a sagittal view of the lateral ventricular wall. The square indicates the region analyzed in A–D. D, dorsal; V, ventral; P, posterior; A, anterior. (A–D) Whole-mount lateral ventricular wall from a P5 (A), P7 (B), P9 (C) and adult (D) mouse was stained for Pcnt (red) and ZO1 (green). (A'–D') Higher magnification of the boxed regions in A–D. At P5, the basal bodies were broadly distributed in the apical membrane of ependymal cells (arrows in A'). (E) Distribution of the centroid in the ciliated areas. The schematic shows a comparison of the centroid position of the cell with the centroid position of the ciliated area. (F) The percentage of cells with the centroid of the ciliated area in the anterior quadrant was significantly higher at P9 than at P7 ( $P=0.0486$ ). (G) The cell area was significantly greater at P9 than P7 or in adult (P7 versus P9,  $P=0.0095$ ; P9 versus adult,  $P<0.001$ ). (H) The area of the ciliated region was significantly smaller at P9 than P7 or in adults (P7 versus P9,  $P<0.001$ ; P9 versus adult,  $P<0.001$ ). Anterior is to the right and ventral to the bottom in all panels. \*,  $P<0.05$ ; \*\*,  $P<0.01$ ; \*\*\*,  $P<0.001$ . Scale bar: 5  $\mu\text{m}$ .

the basal bodies were not as densely packed as at P9. However, they were still asymmetrically distributed, with more in the anterior region of each ependymal cell, in agreement with a recent report on translational polarity (Fig. 1D) (Mirzadeh et al., 2010).

We next compared the centroid position of the area containing basal bodies with that of the whole cell, by dividing each cell into quadrants (dorsal, ventral, posterior, anterior), and we counted the number of cells with a ciliated area centroid that lay in each quadrant (Fig. 1E). In P5 tissue, the basal bodies were dispersed, and the centroid of the ciliated area was found in all four quadrants. From P7 onwards, however, the number of cells with the centroid of the ciliated area in the anterior quadrant was significantly larger than of cells with the centroid in the other three quadrants ( $\chi^2$  analysis; P5, 105 cells; P7, 91 cells; P9, 109 cells; adult, 137 cells; from three mice in each case). The percentage of cells in which the centroid of the ciliated area was in the anterior quadrant peaked at P9 (Fig. 1F). The density of the basal bodies also changed during differentiation. Whereas the cell area was slightly larger at P9 than at P7 and the adult stage (Fig. 1G), the area of the ciliated region was transiently and significantly reduced between P9 and P15 compared with P7 (Fig. 1H; data not shown), suggesting that the basal bodies became highly concentrated at the anterior of the ependymal cells during P9–15. We therefore focused on this period in subsequent experiments. Together, these data show that ependymal cells acquire their translational polarity between P5 and P9.

### Basal bodies move to the anterior region of ependymal cells

To observe how the translational polarity of ependymal cells emerges between P5 and P9, we performed time-lapse recordings of basal bodies in the living ventricular wall. The lateral wall of the lateral ventricle of P5 Cent2GFP transgenic mice, which express a centrin 2-GFP fusion protein that labels the basal body (Higginbotham et al., 2004), was embedded in Matrigel, and the movement of the basal bodies was studied by time-lapse image analysis over 10 hours (Fig. 2; see Movie 1 in the supplementary material). At the beginning of the recording, the basal bodies were broadly distributed at low density in the apical membrane of the ependymal cells (0 min in Fig. 2). All the basal bodies in a single cell migrated simultaneously in this process, and they gradually became asymmetrically distributed and formed a dense accumulation at the anterior apical membrane (Fig. 2; see Movie 1 in the supplementary material). We concluded that the basal bodies change their distribution within the apical membrane of ependymal cells along the A–P axis of the ventricular wall to accumulate in the anterior-most part of the cell membrane.

### Translational polarity and rotational polarity are established at around the same developmental stage

To further characterize the timing of basal body migration during the period of ependymal cilia maturation, we used the two-color imaging of beating cilia and basal bodies to simultaneously observe

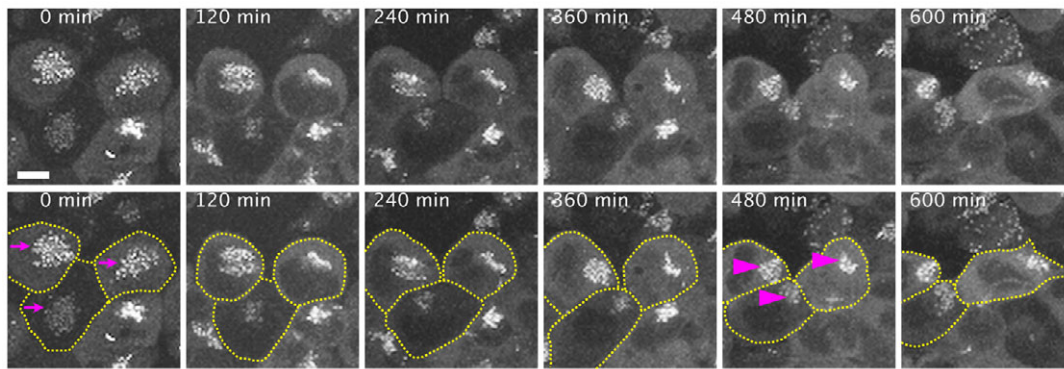


**Fig. 2. Live imaging of basal bodies migrating toward the anterior apical membrane of ependymal cells.** Still images from a time-lapse recording of GFP-labeled basal bodies migrating in the apical membrane of ependymal cells of P5 Cent2GFP mice (see Movie 1 in the supplementary material). The dispersed basal bodies (0 min; arrows) gradually became asymmetrically and densely distributed to the anterior apical membrane of ependymal cells (480 min; arrowheads). The yellow dotted line indicates the cell boundary. Scale bar: 5  $\mu$ m.

the translational and rotational polarities of differentiating cells. In the lateral ventricle of P1 mice, most of the ependymal cells were immature and had non-polarized, short cilia (Fig. 3A), but by P7 the ependymal cells were mature and bore long, polarized cilia (Fig. 3B). To determine whether ciliary beating in immature and mature ependymal cells correlated with basal body localization, we recorded side views of the beating ependymal cilia of Cent2GFP mice. We used P5-7 mice to observe ciliary beating on dispersed basal bodies and P14-19 mice to analyze ciliary beating on anteriorly located basal bodies. To observe the cilia, brain slices were stained with a fluorescent dye and the ciliary beating was recorded using a high-speed confocal microscope.

In immature ependymal cells, in which the basal bodies were distributed broadly in the apical membrane ('dispersed cells'), the ependymal cilia did not beat unidirectionally (Fig. 3C,F; see Movie 2 in the supplementary material), consistent with TEM observations of fixed samples, which show a random alignment of the basal bodies at this stage (Guirao et al., 2010). By contrast, the ependymal cilia on cells with anteriorly located basal bodies ('localized' cells) showed coordinated beating in the anterior direction (Fig. 3D,F; see Movie 2 in the supplementary material). The percentage of cells with anteriorly directed ciliary beating was significantly greater for the localized than the dispersed cells (Fig. 3G) (dispersed, 43 cells; localized, 28 cells; both from four mice). In addition, the cilia on localized cells were longer than on dispersed cells (Fig. 3H) (dispersed, 39 cilia; localized, 53 cilia; both from three mice). To quantify the functional maturation of the cilia, we calculated the ciliary beat frequency (CBF) of these cells. The CBF was higher in the localized cells than in dispersed cells (Fig. 3I) (18 cells from three mice for both dispersed and localized). Thus, translational polarity was evident in the ependymal cells in which the rotational polarity was established, and at around the same developmental stage.

### PCP signals regulate the rotational, but not the translational, polarity in ependymal cells

We recently found that when primary cultured ependymal cells were exposed to artificial shear flow during their maturation, their cilia were reoriented to reflect the flow direction via the PCP protein Vangl2 located in the ciliary axoneme (Guirao et al., 2010), suggesting that fluid flow and PCP signaling both play important roles in establishing the rotational polarity of ependymal cilia. Here, we examined whether fluid flow and PCP signaling are also

involved in the translational polarity of ependymal cilia. To test the role of fluid flow in the establishment of translational polarity, we compared the distribution of basal bodies between cultures with and without flow. The basal bodies of ependymal cells cultured with flow did not show a polarized distribution along the direction of flow (Fig. 4A-D). This suggested that fluid flow alone is not sufficient to induce translational planar polarity of basal bodies in primary culture.

Next, we examined the involvement of PCP signaling in the establishment of translational polarity. Immunostaining of the Cent2GFP ventricular wall revealed that Dvl2 accumulated at high levels near the basal bodies in differentiating ependymal cells (Fig. 4E). A similar localization of Dvl has been reported for *Xenopus* larvae (Park et al., 2008). Double immunostaining with R4109, a ciliary rootlet marker (Hagiwara et al., 2000), indicated that the Dvl2 was localized to the ciliary rootlets (Fig. 4F). To assess the role of Dvl2 in planar polarity formation in ependymal cells, we used a deletion construct, Dvl2 $\Delta$ PDZ, that lacks the PDZ domain (Habas et al., 2001), and Dvl2-C, which contains only the conserved C-terminus of Dvl2. These constructs function as dominant-negative forms of Dvl2 that inhibit the PCP signal (Park et al., 2008) (Fig. 4G).

First, to test whether the inhibition of Dvl2 would affect rotational polarity in vitro, cultured ependymal cells were transfected with plasmids encoding a Dvl2-C-GFP or Dvl2 $\Delta$ PDZ-GFP fusion protein. We then labeled the cilia with a fluorescent dye and performed high-speed confocal imaging. The ciliary beating of the single control cells was unidirectional, as shown in our previous report (Guirao et al., 2010), whereas that in cells transfected with one of the dominant-negative forms of Dvl2 was disturbed (see Movies 4-6 in the supplementary material). To quantify the ciliary orientation, we added small fluorescent latex beads to the medium. The movement of beads attached to the cilia was traced and is shown as lines indicating the trajectory of ciliary beating (Fig. 4H-J; see Movies 7-9 in the supplementary material). The beating direction of the cilia was quantified by measuring the angle to the mean angle in each cell, using the trace image made by the fluorescent beads. The coordinated ciliary beating was disturbed in both the Dvl2- $\Delta$ PDZ-GFP-expressing and Dvl2-C-GFP-expressing cells (Fig. 4K) (control, 147 cilia from 18 cells; Dvl2 $\Delta$ PDZ, 80 cilia from 11 cells; Dvl2-C-GFP, 49 cilia from six cells), suggesting that Dvl2 is required for rotational polarity in ependymal cells generated in vitro.

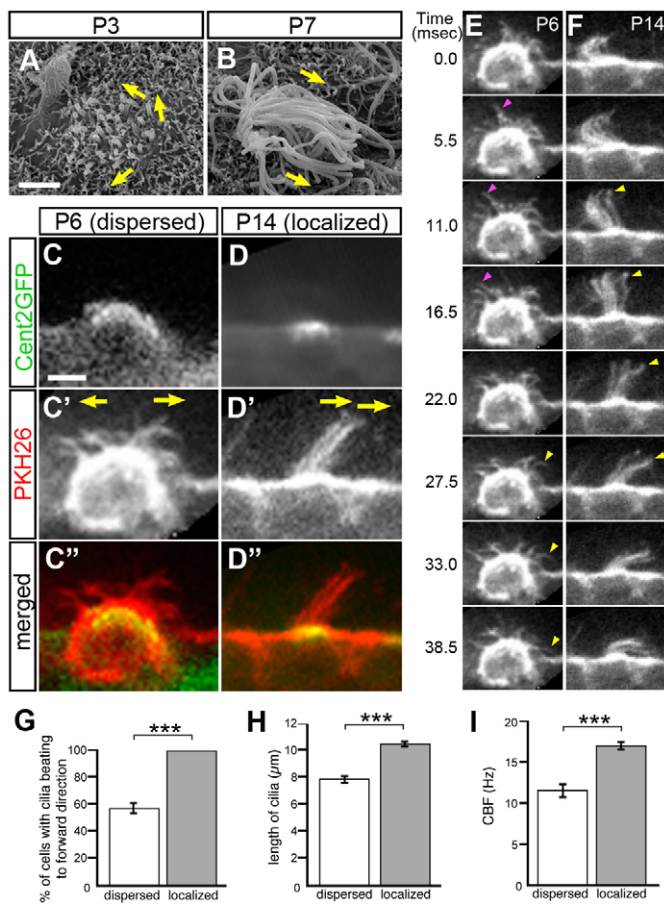


**Fig. 3. Translational and rotational polarity are established at around the same developmental stage.** (A,B) Scanning electron microscopy of the ventricular surface at P3 (A) and P7 (B). Arrows indicate ciliary orientation. (C,D) Lateral views of ependymal cells from P5 (C) and P14 (D) Cent2GFP mice. (C',D') Beating cilia labeled with PKH26, a fluorescent dye. Arrows indicate the ciliary beating direction. (C'',D'') Merged images of Cent2GFP and PKH26. (E,F) Series of still images from a high-speed recording (see Movies 2 and 3 in the supplementary material) of the beating cilia of ependymal cells (as shown in C,D). Cilia beating to the anterior (E,F) and posterior (E) directions are indicated by yellow and magenta arrowheads, respectively. (G) The percentage of cells with cilia beating in the forward direction was significantly greater among cells with anteriorly localized basal bodies ('localized') than among those with dispersed basal bodies ('dispersed') ( $P < 0.001$ ). (H) The cilia were significantly longer in the localized than dispersed cells ( $P < 0.001$ ). (I) The ciliary beat frequency (CBF) was significantly higher in the localized than dispersed cells ( $P < 0.001$ ). \*\*\*,  $P < 0.001$ . Scale bars: 2 μm in A,B; 5 μm in C,D.

Next, to examine the effect of inhibiting Dvl2 on the differentiation of ependymal cells *in vivo*, a lentivirus expression vector for Dvl2ΔPDZ-GFP was injected into the lateral ventricle of neonatal mice, and the brains were fixed at P10. Staining with a cilium marker revealed that ciliogenesis was not impaired in the Dvl2ΔPDZ-GFP-expressing cells (data not shown). By performing immunoelectron microscopy using GFP-positive cells, the ciliary orientation was quantified based on the orientation of the basal foot, which protrudes laterally from the basal body in the direction of the effective stroke of the ciliary beat (Boisvieux-Ulrich and Sandoz, 1991). We found that the ciliary orientation was disturbed in the Dvl2ΔPDZ-GFP-expressing cells compared with controls

(Fig. 4L-O) (CSD value: control,  $21.3 \pm 5.6^\circ$ , four cells from two mice; Dvl2ΔPDZ,  $55.1 \pm 9.3^\circ$ , five cells from three mice). These results suggested that Dvl2 is necessary for the establishment of rotational polarity, consistent with previous reports that PCP components are required for this polarity (Guirao et al., 2010; Tissir et al., 2010).

Next, we examined whether the inhibition of Dvl2 also affects the translational polarity of the basal bodies. The number of cells with the centroid of the ciliated area in the anterior quadrant was not affected in Dvl2ΔPDZ-expressing cells (Fig. 4P-R) (control, 21 cells from three mice; Dvl2ΔPDZ, 29 cells from five mice). This indicated that the PCP pathway regulates the rotational, but not the translational, polarity of the basal bodies in ependymal cells.

### Non-muscle myosin regulates the translational, but not the rotational, polarity of basal bodies

Emerging evidence suggests that NMII regulates planar polarity formation in several tissues in mammals. To examine whether NMII is involved in the planar polarity of basal bodies, we first analyzed the expression pattern of the NMHCs in differentiating ependymal cells. In mammals, three NMHC isoforms have been identified: Myh9, Myh10 and Myh14. Myh9 was highly expressed and broadly distributed in the ependymal cells, but it was not detectable in neural stem cells with primary cilia (Fig. 5A). Myh10 and Myh14 were distributed in the cytoplasm of ependymal cells and highly localized in the vicinity of basal bodies (Fig. 5B,C). At the apical surface of cells, the localization of Myh14 in the vicinity of basal bodies was even more evident (Fig. 5D). The activity of NMII is regulated mainly by the phosphorylation of its RLCs by Rho-associated protein kinase (ROCK; Rock1 and Rock2 – Mouse Genome Informatics) and myosin light chain kinase (MLCK; Mylk – Mouse Genome Informatics) (Adelstein and Conti, 1975; Amano et al., 1996). We therefore examined myosin activation using an antibody specific for the phosphorylated form of myosin light chain (pMLC), and found that the pMLC signal was localized to the vicinity of basal bodies (Fig. 5E). Thus, NMII was highly expressed and activated in differentiating ependymal cells, indicating that NMII could be involved in the planar polarization of ependymal cilia.

To determine whether NMII plays a role in basal body distribution, we examined the effects of three small-molecule inhibitors: blebbistatin, which inhibits myosin II (Straight et al., 2003); ML-9, which inhibits MLCK (Saitoh et al., 1987); and Y27632, which inhibits ROCK (Uehata et al., 1997). We injected the inhibitors or vehicle alone into the lateral ventricles of P5 mice and fixed the brains at P10. In the control animals, the basal bodies accumulated in the anterior region of the ependymal cells (Fig. 6A). The basal bodies were dispersed in the apical membrane of the ependymal cells in brains injected with blebbistatin or ML-9 as compared with mock-injected controls (Fig. 6A-C), but Y27632 did not affect basal body distribution (Fig. 6D). The treatment with blebbistatin or ML-9 significantly decreased the number of cells with anteriorly localized basal bodies in a dose-dependent manner (control for blebbistatin and ML-9, 172 cells from five mice; lower-dose blebbistatin, 142 cells from four mice; higher-dose blebbistatin, 65 cells from four mice; lower-dose ML-9, 158 cells from five mice; higher-dose ML-9, 157 cells from five mice; control for Y27632, 51 cells from three mice; Y27632, 45 cells from three mice) (Fig. 6I). In these experiments, staining for acetylated tubulin showed that the cilia were elongated in the inhibitor-treated brains, indicating that ciliogenesis was largely

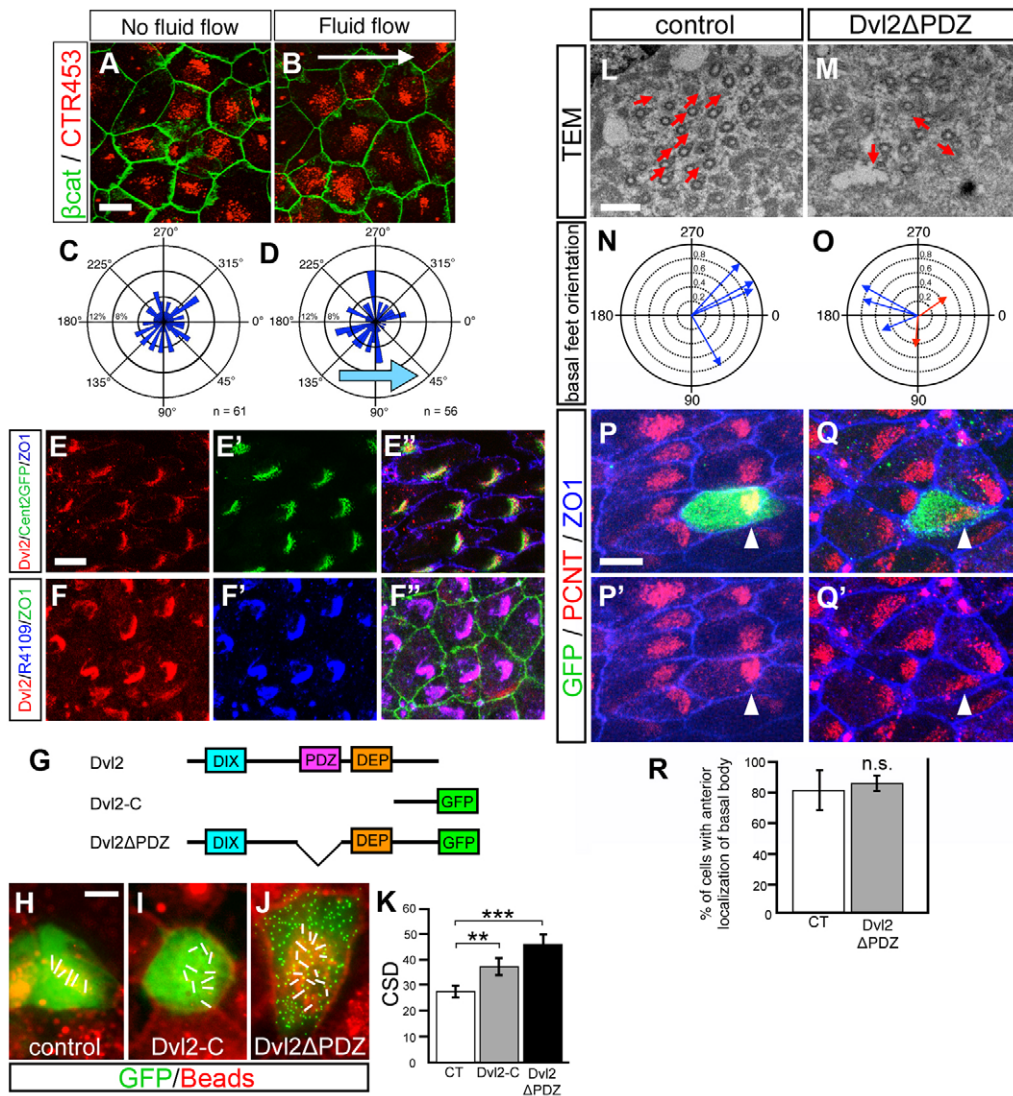


**Fig. 4. Inhibition of the PCP signal affects the rotational, but not the translational, polarity of basal bodies in ependymal cells.** (A,B) Primary culture of ependymal cells cultured without (A) or with (B) external fluid flow and stained with CTR453 (basal body, red) and  $\beta$ -catenin (green) antibodies. (C,D) Scoring of the basal body distribution in ependymal cells cultured without (C) or with (D) external flow. The applied external flow direction in the culture is indicated (light-blue arrow). In both conditions, the distribution of basal bodies was statistically uniform (Rayleigh's test; without flow,  $P=0.938$ ; with flow,  $P=0.253$ ). (E-E'') Ependymal cells from a Cent2GFP mouse immunostained for Dvl2 (red) and ZO1 (blue). (F-F'') Ependymal cells stained for Dvl2 (red), R4109 (ciliary rootlet, blue) and ZO1 (green). (G) The wild-type and mutant Dvl2 constructs used in this study. (H-J) Direction of ciliary beating revealed by fluorescent beads (lines) in cultured ependymal cells transfected with control (H; see Movie 7 in the supplementary material) and dominant-negative forms of Dvl2, Dvl2-C (I; see Movie 8 in the supplementary material) and Dvl2 $\Delta$ PDZ (J; see Movie 9 in the supplementary material). (K) The circular standard deviation (CSD) was significantly greater in the Dvl2-C-expressing and Dvl2 $\Delta$ PDZ-expressing cells than in the controls (control versus Dvl2-C,  $P=0.0107$ ; control versus Dvl2 $\Delta$ PDZ,  $P<0.001$ ). (L,M) TEM analyses of the basal foot alignment in control (L) and Dvl2 $\Delta$ PDZ-expressing (M) ependymal cells. The directions of the basal feet are indicated by red arrows. (N,O) Circular plots depicting the basal foot circular distributions in control (N) and Dvl2 $\Delta$ PDZ-expressing (O) cells. The basal foot circular distributions within each cell were plotted and are represented by red arrows for a statistically uniform distribution (Rayleigh's test;  $P>0.05$ ) and blue arrows for a non-uniform distribution. (P-Q'') Ependymal cells transfected with lentivirus control vector (P) or expressing Dvl2 $\Delta$ PDZ (Q) were stained for GFP (green), Pcnt (red) and ZO1 (blue). Anteriorly localized basal bodies are indicated by arrowheads. (R) No significant difference was found in the number of cells with the centroid of the ciliated area in the anterior quadrant between the control and Dvl2 $\Delta$ PDZ groups ( $P=0.8782$ ). \*\*,  $P<0.01$ ; \*\*\*,  $P<0.001$ . Scale bars: 10  $\mu$ m in A,B,E-F'',H-J,P-Q'; 2  $\mu$ m in L,M.

maintained (Fig. 6E-H). These results suggested that the activation of NMII via MLCK is important for the establishment of translational polarity.

Next, to examine whether the inhibition of NMII disturbs the ciliary beating pattern, we recorded side views of the beating ependymal cilia using mock- or blebbistatin-injected Cent2GFP

mice. We did not detect any obvious abnormality in the orientation (see Movies 10, 11 in the supplementary material) or frequency of the ciliary beating (control,  $19.1\pm 0.87$  Hz, 22 cilia from three mice; blebbistatin,  $19.0\pm 1.05$  Hz, 25 cilia from three mice;  $P=0.9254$ ) in tissues from mice treated with blebbistatin, indicating that the inhibition of NMII did not affect ciliary beating. These results

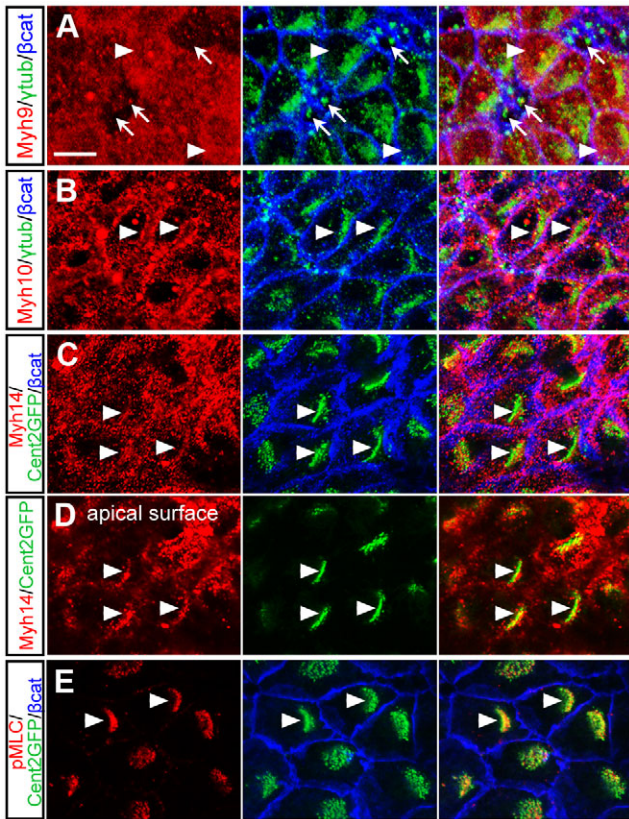


**Fig. 5. Distribution of Myh9, Myh10, Myh14 and pMLC in differentiating ependymal cells.** (A, B) Ependymal cells were stained for Myh9 (A) and Myh10 (B) (red) together with  $\gamma$ -tubulin (green) and  $\beta$ -catenin (blue). (A) Myh9 was highly expressed and broadly distributed in the ependymal cells (arrowheads), but was not detectable in neural stem cells with primary cilia (arrows). (B) Myh10 was distributed in the cytoplasm of ependymal cells and located close to the basal bodies (arrowheads). (C, D) Ependymal cells of Cent2GFP mice were stained for Myh14 (red) together with  $\beta$ -catenin (blue). (C) Myh14 was detected in the vicinity of basal bodies (C, arrowheads) and in the cytosol. (D) At the apical surface (same cells as C), the localization of Myh14 in the vicinity of basal bodies was even more evident (D, arrowheads). (E) Ependymal cells of Cent2GFP mice were stained for pMLC (red) together with  $\beta$ -catenin (blue). pMLC was closely associated with the basal bodies (arrowheads). Scale bar: 10  $\mu$ m.

indicated that NMII regulates the translational, but not the rotational, polarity of the basal body and that these two polarities are determined by independent mechanisms.

To further examine the role of NMII in the establishment of translational polarity, knockdown experiments with vector-based RNAi were performed. Plasmids containing knockdown target sequences for *Myh9*, *Myh10* and *Myh14*, or *lacZ* (as a negative control), together with DsRed-Express were introduced into the lateral ventricles of P1 mice by electroporation and the brains fixed at  $\sim$ P12. Immunostaining for Myh9, Myh10 and Myh14 was efficiently reduced in the DsRed-Express-positive cells in the NMII-knockdown samples compared with the controls (see Fig. S1 in the supplementary material). The basal bodies docked normally at the apical membrane of the NMII-knockdown cells (Fig. 6J', J'', M', M''), and the DsRed-Express signal was detected in the ciliary axonemes in the NMII-knockdown cells, as in the controls (Fig. 6L, O), suggesting that the extension of the ciliary axonemes

was not notably affected by the knockdown of NMII. However, in the Myh9/Myh10/Myh14-knockdown ependymal cells, the basal bodies were dispersed in the apical membrane (Fig. 6J, K, M, N) and the number of cells with anteriorly localized basal bodies was significantly decreased (control, 29 cells from five mice; NMII knockdown, 32 cells from three mice) (Fig. 6P). This result suggested that NMII regulates the distribution of basal bodies and the establishment of the translational polarity of ependymal cells in a cell-autonomous manner.

## DISCUSSION

### Basal bodies migrate within the apical cell membrane of differentiating ependymal cells after docking

The results presented here demonstrate that ependymal cells acquire translational polarity by the migration of basal bodies to the anterior of the apical cell membrane. For this study, we developed a method for time-lapse imaging of the cultured, whole-mount lateral wall of the lateral ventricle by modifying conventional methods for brain slice culture. Using this approach, we found that the dispersed basal bodies moved towards, and accumulated at, the anterior edge of the ependymal cells within 10 hours. Live imaging also revealed that all the basal bodies in a single cell migrate simultaneously. Thus, our time-lapse imaging of fluorescently labeled basal bodies clearly revealed their behavior after docking, providing the first evidence that basal bodies indeed move towards the anterior border of the apical membrane of ependymal cells along the A-P axis of the brain.

What is the functional significance of the translational polarity of ependymal cells? The normal beating behavior of the dispersed cilia on ependymal cells after treatment with an inhibitor of NMHCs suggested that translational polarity is dispensable for the directional and rapid beating of cilia (see Movies 10-11 in the supplementary material). Since the anterior positioning of the basal bodies causes a posterior tilt of nodal cilia, which produces a leftward flow (Nonaka et al., 2005; Okada et al., 2005), the anterior localization of the ependymal cilia might also affect the generation of fluid flow. The basal bodies did not exhibit translational polarity in other multiciliated cells, such as those of the trachea and oviduct (data not shown), suggesting that it is a unique feature of ependymal cells. Differences in the viscosity and amount of fluid might account for the differences in the alignment pattern of the basal bodies in these cells. The viscosity of cerebrospinal fluid (CSF) is lower than that of the mucus in the oviduct or trachea, and the amount of liquid is different: the lateral ventricles are filled with CSF, whereas only the epithelial surfaces of the trachea and oviduct are covered with mucus, which exists as a thin layer.

### PCP signals regulate the rotational, but not the translational, polarity of basal bodies

Our recent study indicated that the orientation of ependymal cilia is regulated by the PCP protein Vangl2 (Guirao et al., 2010). It was also recently reported that the PCP components Celsr2 and Celsr3, which are members of the non-classical cadherin family, are involved in establishing rotational polarity and the membrane distribution of Vangl2 in ependymal cells (Tissir et al., 2010). Here, we found that the inhibition of Dvl2, a cytoplasmic effector of the PCP pathway, also disturbs rotational polarity. The proper membrane distribution of Dvl2 depends on the function of Vangl2 in the inner ear (Wang et al., 2005). It is possible that these three PCP components (Celsr proteins, Vangl2 and Dvl2) act cooperatively to establish the rotational polarity of ependymal cilia. By contrast, we found that translational polarity was not affected

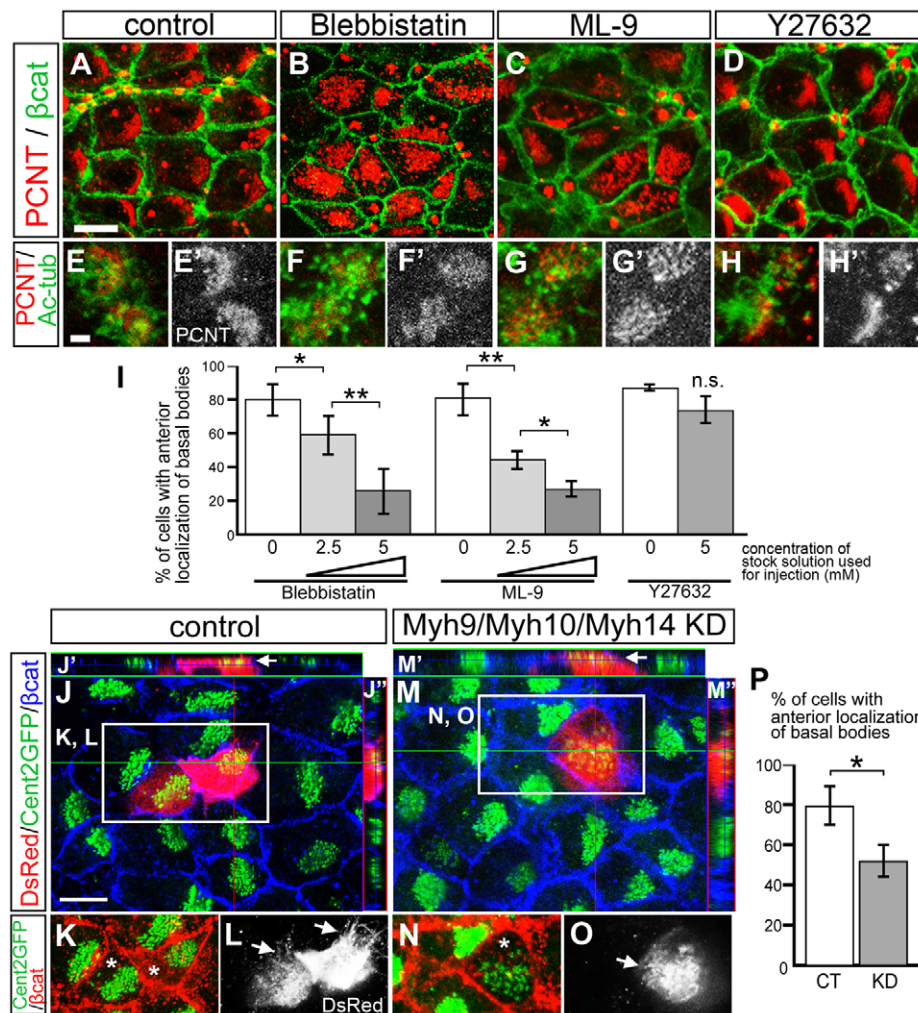


**Fig. 6. Inhibition of NMII disrupts the translational, but not the rotational, polarity of the basal bodies in ependymal cells.**

(A-H') Vehicle control (A,E) or inhibitors of NMII (B,F; higher dose blebbistatin), MLCK (C,G; higher dose ML-9) or ROCK (D,H; Y27632) were injected into the lateral ventricles of P5 mice. Five days after injection, the ependymal cells were immunostained for Pcnt (red) and  $\beta$ -catenin (green) (A-D) or acetylated tubulin (green in E-H, white in E'-H'). (I) Injection of blebbistatin or ML-9 resulted in a significant and dose-dependent decrease in the number of cells with the centroid of the ciliated area in the anterior quadrant. By contrast, Y27632 did not affect the anterior localization of the basal bodies.  $P < 0.05$ , control versus lower dose blebbistatin;  $P < 0.01$ , lower dose blebbistatin versus higher dose blebbistatin;  $P < 0.01$ , control versus lower dose ML-9;  $P < 0.05$ , lower dose ML-9 versus higher dose ML-9;  $P = 0.0186$ , control versus Y27632. (J-O) Knockdown of NMII. Ependymal cells from Cent2GFP mice electroporated with plasmids expressing a control (J-L) or a Myh9/Myh10/Myh14-knockdown (KD) vector (M-O) that co-expressed DsRed (red) were stained with  $\beta$ -catenin (blue). (J',J'',M',M'') Three-dimensional reconstruction images. Basal bodies in the apical cell membrane of DsRed-expressing cells are indicated by arrows (J',M'). (K,N)  $\beta$ -catenin (pseudocolored red) and Cent2GFP (green) signal in the boxed regions indicated in J and M. DsRed-expressing cells are indicated by asterisks. (L,O) DsRed-labeled cilia (arrows) in the boxed regions indicated in J and M. (P) The number of cells with the centroid of the ciliated area in the anterior quadrant was significantly reduced in the Myh9/Myh10/Myh14-KD samples compared with controls (CT) ( $P = 0.0316$ ). \*,  $P < 0.05$ ; \*\*,  $P < 0.01$ . Scale bars: 10  $\mu$ m in A-D,J-O; 2  $\mu$ m in E-H'.

by the inhibition of Dvl2. The PCP pathway is known to regulate various cellular processes through the activation of ROCK and JNK (Mapk8 – Mouse Genome Informatics). We found that the pharmacological inhibition of both of these kinases did not affect translational polarity (Fig. 6D; data not shown), similar to the lack of effect from inhibiting Dvl2. Together, our results suggest that translational polarity is not regulated by the PCP signaling pathway, although PCP signaling does regulate rotational polarity (Guirao et al., 2010; Tissir et al., 2010); therefore, these two planar polarities are regulated by distinct molecular mechanisms.

Recent papers have reported that the PCP pathway regulates the position of the basal bodies of nodal cilia in mice and zebrafish (Antic et al., 2010; Hashimoto et al., 2010; Borovina et al., 2010).

Similarly, PCP signaling is important for the polarization of the primary cilium, or kinocilium, in the hair cells of the organ of Corti (Curtin et al., 2003; Montcouquiou et al., 2003; Wang et al., 2005; Wang et al., 2006), suggesting that the PCP pathway is required for positioning primary cilia but not the multiple cilia of ependymal cells. In addition, cilia are required for the normal positioning of the basal body of the kinocilium (Jones et al., 2008) but not the basal body of ependymal cilia (Mirzadeh et al., 2010). In contrast to the single basal body of nodal cells or hair cells, the basal bodies of ependymal cilia migrate in a group and over a longer distance during translational polarization. It is possible that these differences account for the different requirements for PCP signaling in basal body positioning.

## NMII regulates the translational polarity of basal bodies in differentiating ependymal cells

In this study, we showed that the inhibition of NMII greatly disturbs translational polarity, indicating that NMII is required for the anterior migration of basal bodies in the apical membrane of ependymal cells. Recently, the NMII motor was shown to be important for controlling the movement of the centrosome, which is identical to the basal body, into the leading process of migrating neurons (Solecki et al., 2009). Thus, it is reasonable that NMII would regulate the movement of the basal bodies in ependymal cells.

It is still unclear what signal activates NMII regulation of basal body migration. Our inhibitor experiments suggested that the activation of NMII by MLCK is important for translational polarity. An increase in the intracellular calcium concentration initiates smooth muscle contraction through the phosphorylation of RLC by MLCK downstream of the calcium/calmodulin signal in several tissues, including the renal collecting duct (Chou et al., 2004). Previous studies indicate that the calcium/calmodulin-dependent protein kinase II and calmodulin superfamily proteins are expressed in ependymal cells (Fukunaga et al., 1988; Maillieux et al., 1993), suggesting that calmodulin signaling in these cells could activate NMII to establish the translational polarity.

In conclusion, the results presented here demonstrate that basal bodies migrate anteriorly in the apical membrane and establish the translational polarity of ependymal cells. Taking into consideration recent findings (Guirao et al., 2010; Mirzadeh et al., 2010; Tissir et al., 2010) and our present results, the two distinct polarities are probably formed during ependymal cell differentiation as follows. In neonates, the formation of rotational polarity is triggered by fluid flow (Guirao et al., 2010), possibly generated by the secretion of CSF from the choroid plexus and its absorption in the foramen of Monroe in the lateral ventricles, via mechanisms involving motile cilia and PCP signaling (Guirao et al., 2010; Tissir et al., 2010) (Fig. 4). By contrast, translational polarization is initiated by the anterior localization of the basal body of the primary cilia of radial glial cells (Mirzadeh et al., 2010) and is established after the transformation of radial glial cells to ependymal cells by the anterior migration of the basal bodies (Figs 1-3). These two polarities are determined independently by distinct cellular and molecular mechanisms (Fig. 4). Our results identify NMII as a key regulator of translational planar polarity (Figs 5, 6) and provide new insight into how this PCP is established in multiciliated tissue.

### Acknowledgements

We are grateful to R. Habas, H. Miyoshi, H. Hagiwara and J. G. Gleeson for providing materials; and I. Miyoshi, H. Hamada, M. Hashimoto, S. Shimada, Y. Yu and H. Naka for technical advice. This work was supported by the Human Frontier Science Program, the Ministry of Education, Culture, Sports, Science and Technology, the Ministry of Health, Labor and Welfare, the Japan Society for the Promotion of Science, CREST (JST), the Toray Science Foundation, the Mitsubishi Foundation, the Japan Science Society, and the Hayashi Memorial Foundation for Female Natural Scientists.

### Competing interests statement

The authors declare no competing financial interests.

### Supplementary material

Supplementary material for this article is available at <http://dev.biologists.org/lookup/suppl/doi:10.1242/dev.050120/-/DC1>

### References

- Adelstein, R. S. and Conti, M. A. (1975). Phosphorylation of platelet myosin increases actin-activated myosin ATPase activity. *Nature* **256**, 597-598.
- Amano, M., Ito, M., Kimura, K., Fukata, Y., Chihara, K., Nakano, T., Matsuura, Y. and Kaibuchi, K. (1996). Phosphorylation and activation of myosin by Rho-associated kinase (Rho-kinase). *J. Biol. Chem.* **271**, 20246-20249.
- Antic, D., Stubbs, J. L., Suyama, K., Kintner, C., Scott, M. P. and Axelrod, J. D. (2010). Planar cell polarity enables posterior localization of nodal cilia and left-right axis determination during mouse and *Xenopus* embryogenesis. *PLoS One* **5**, e8999.
- Bailey, E., Doree, M., Nurse, P. and Bornens, M. (1989). p34cdc2 is located in both nucleus and cytoplasm; part is centrosomally associated at G2/M and enters vesicles at anaphase. *EMBO J.* **8**, 3985-3995.
- Bertet, C., Sulak, L. and Lecuit, T. (2004). Myosin-dependent junction remodelling controls planar cell intercalation and axis elongation. *Nature* **429**, 667-671.
- Boisvieux-Ulrich, E. and Sandoz, D. (1991). Determination of ciliary polarity precedes differentiation in the epithelial cells of quail oviduct. *Biol. Cell* **72**, 3-14.
- Borovina, A., Superina, S., Voskas, D. and Ciruna, B. (2010). Vangl2 directs the posterior tilting and asymmetric localization of motile primary cilia. *Nat. Cell Biol.* **12**, 407-412.
- Boutin, C., Diestel, S., Desoeuvre, A., Tiveron, M. C. and Cremer, H. (2008). Efficient in vivo electroporation of the postnatal rodent forebrain. *PLoS ONE* **3**, e1883.
- Chou, C. L., Christensen, B. M., Frische, S., Vorum, H., Desai, R. A., Hoffert, J. D., de Lanerolle, P., Nielsen, S. and Knepper, M. A. (2004). Non-muscle myosin II and myosin light chain kinase are downstream targets for vasopressin signaling in the renal collecting duct. *J. Biol. Chem.* **279**, 49026-49035.
- Curtin, J. A., Quint, E., Tshipouri, V., Arkell, R. M., Cattanach, B., Copp, A. J., Henderson, D. J., Spurr, N., Stanier, P., Fisher, E. M. et al. (2003). Mutation of *Celsr1* disrupts planar polarity of inner ear hair cells and causes severe neural tube defects in the mouse. *Curr. Biol.* **13**, 1129-1133.
- Fukunaga, K., Goto, S. and Miyamoto, E. (1988). Immunohistochemical localization of  $Ca^{2+}$ /calmodulin-dependent protein kinase II in rat brain and various tissues. *J. Neurochem.* **51**, 1070-1078.
- Ganner, A., Lienkamp, S., Schafer, T., Romaker, D., Wegierski, T., Park, T. J., Spreitzer, S., Simons, M., Gloy, J., Kim, E. et al. (2009). Regulation of ciliary polarity by the APC/C. *Proc. Natl. Acad. Sci. USA* **106**, 17799-17804.
- Guirao, B., Meunier, A., Mortaud, S., Aguilera, A., Corsi, J. M., Strehl, L., Hirota, Y., Desoeuvre, A., Boutin, C., Han, Y. G. et al. (2010). Coupling between hydrodynamic forces and planar cell polarity orients mammalian motile cilia. *Nat. Cell Biol.* **12**, 341-350.
- Habas, R., Kato, Y. and He, X. (2001). Wnt/Frizzled activation of Rho regulates vertebrate gastrulation and requires a novel Formin homology protein Daam1. *Cell* **107**, 843-854.
- Hagiwara, H., Aoki, T., Ohwada, N. and Fujimoto, T. (2000). Identification of a 195 kDa protein in the striated rootlet: its expression in ciliated and ciliogenic cells. *Cell Motil. Cytoskeleton* **45**, 200-210.
- Hashimoto, M., Shinohara, K., Wang, J., Ikeuchi, S., Yoshida, S., Meno, C., Nonaka, S., Takada, S., Hatta, K., Wynshaw-Boris, A. et al. (2010). Planar polarization of node cells determines the rotational axis of node cilia. *Nat. Cell Biol.* **12**, 170-176.
- Higginbotham, H., Bielas, S., Tanaka, T. and Gleeson, J. G. (2004). Transgenic mouse line with green-fluorescent protein-labeled Centrin 2 allows visualization of the centrosome in living cells. *Transgenic Res.* **13**, 155-164.
- Hirota, Y., Ohshima, T., Kaneko, N., Ikeda, M., Iwasato, T., Kulkarni, A. B., Mikoshiba, K., Okano, H. and Sawamoto, K. (2007). Cyclin-dependent kinase 5 is required for control of neuroblast migration in the postnatal subventricular zone. *J. Neurosci.* **27**, 12829-12838.
- Jones, C., Roper, V. C., Foucher, I., Qian, D., Banizs, B., Petit, C., Yoder, B. K. and Chen, P. (2008). Ciliary proteins link basal body polarization to planar cell polarity regulation. *Nat. Genet.* **40**, 69-77.
- Kojima, T., Hirota, Y., Ema, M., Takahashi, S., Miyoshi, I., Okano, H. and Sawamoto, K. (2010). Subventricular zone-derived neural progenitor cells migrate along a blood vessel scaffold toward the post-stroke striatum. *Stem Cells* **28**, 545-554.
- Ma, X., Bao, J. and Adelstein, R. S. (2007). Loss of cell adhesion causes hydrocephalus in nonmuscle myosin II-B-ablated and mutated mice. *Mol. Biol. Cell* **18**, 2305-2312.
- Maillieux, P., Halleux, P., Verslijpe, M., Segers, V. and Vanderhaeghen, J. J. (1993). Neuronal localization in the rat brain of the messenger RNA encoding calyphosine, a new calcium-binding protein. *Neurosci. Lett.* **153**, 125-130.
- Mirzadeh, Z., Han, Y. G., Soriano-Navarro, M., Garcia-Verdugo, J. M. and Alvarez-Buylla, A. (2010). Cilia organize ependymal planar polarity. *J. Neurosci.* **30**, 2600-2610.
- Mitchell, B., Jacobs, R., Li, J., Chien, S. and Kintner, C. (2007). A positive feedback mechanism governs the polarity and motion of motile cilia. *Nature* **447**, 97-101.
- Mitchell, B., Stubbs, J. L., Huisman, F., Taborek, P., Yu, C. and Kintner, C. (2009). The PCP pathway instructs the planar orientation of ciliated cells in the *Xenopus* larval skin. *Curr. Biol.* **19**, 924-929.

- Miyoshi, H., Blomer, U., Takahashi, M., Gage, F. H. and Verma, I. M. (1998). Development of a self-inactivating lentivirus vector. *J. Virol.* **72**, 8150-8157.
- Montcouquiol, M., Rachel, R. A., Lanford, P. J., Copeland, N. G., Jenkins, N. A. and Kelley, M. W. (2003). Identification of Vangl2 and Scrb1 as planar polarity genes in mammals. *Nature* **423**, 173-177.
- Niwa, H., Yamamura, K. and Miyazaki, J. (1991). Efficient selection for high-expression transfectants with a novel eukaryotic vector. *Gene* **108**, 193-199.
- Nonaka, S., Yoshida, S., Watanabe, D., Ikeuchi, S., Goto, T., Marshall, W. F. and Hamada, H. (2005). De novo formation of left-right asymmetry by posterior tilt of nodal cilia. *PLoS Biol.* **3**, e268.
- Okada, Y., Takeda, S., Tanaka, Y., Belmonte, J. C. and Hirokawa, N. (2005). Mechanism of nodal flow: a conserved symmetry breaking event in left-right axis determination. *Cell* **121**, 633-644.
- Park, T. J., Mitchell, B. J., Abitua, P. B., Kintner, C. and Wallingford, J. B. (2008). Dishevelled controls apical docking and planar polarization of basal bodies in ciliated epithelial cells. *Nat. Genet.* **40**, 871-879.
- Saitoh, M., Ishikawa, T., Matsushima, S., Naka, M. and Hidaka, H. (1987). Selective inhibition of catalytic activity of smooth muscle myosin light chain kinase. *J. Biol. Chem.* **262**, 7796-7801.
- Sawamoto, K., Wichterle, H., Gonzalez-Perez, O., Cholfin, J. A., Yamada, M., Spassky, N., Murcia, N. S., Garcia-Verdugo, J. M., Marin, O., Rubenstein, J. L. et al. (2006). New neurons follow the flow of cerebrospinal fluid in the adult brain. *Science* **311**, 629-632.
- Skoglund, P., Rolo, A., Chen, X., Gumbiner, B. M. and Keller, R. (2008). Convergence and extension at gastrulation require a myosin IIB-dependent cortical actin network. *Development* **135**, 2435-2444.
- Solecki, D. J., Trivedi, N., Govak, E. E., Kerekes, R. A., Gleason, S. S. and Hatten, M. E. (2009). Myosin II motors and F-actin dynamics drive the coordinated movement of the centrosome and soma during CNS glial-guided neuronal migration. *Neuron* **63**, 63-80.
- Straight, A. F., Cheung, A., Limouze, J., Chen, I., Westwood, N. J., Sellers, J. R. and Mitchison, T. J. (2003). Dissecting temporal and spatial control of cytokinesis with a myosin II inhibitor. *Science* **299**, 1743-1747.
- Tissir, F., Qu, Y., Montcouquiol, M., Zhou, L., Komatsu, K., Shi, D., Fujimori, T., Labeau, J., Tyteca, D., Courtoy, P. et al. (2010). Lack of cadherins Celsr2 and Celsr3 impairs ependymal ciliogenesis, leading to fatal hydrocephalus. *Nat. Neurosci.* **13**, 700-707.
- Uehata, M., Ishizaki, T., Satoh, H., Ono, T., Kawahara, T., Morishita, T., Tamakawa, H., Yamagami, K., Inui, J., Maekawa, M. et al. (1997). Calcium sensitization of smooth muscle mediated by a Rho-associated protein kinase in hypertension. *Nature* **389**, 990-994.
- Wang, J., Mark, S., Zhang, X., Qian, D., Yoo, S. J., Radde-Gallwitz, K., Zhang, Y., Lin, X., Collazo, A., Wynshaw-Boris, A. et al. (2005). Regulation of polarized extension and planar cell polarity in the cochlea by the vertebrate PCP pathway. *Nat. Genet.* **37**, 980-985.
- Wang, Y., Guo, N. and Nathans, J. (2006). The role of Frizzled3 and Frizzled6 in neural tube closure and in the planar polarity of inner-ear sensory hair cells. *J. Neurosci.* **26**, 2147-2156.
- Yamamoto, N., Okano, T., Ma, X., Adelstein, R. S. and Kelley, M. W. (2009). Myosin II regulates extension, growth and patterning in the mammalian cochlear duct. *Development* **136**, 1977-1986.
- Yamashita, T., Ninomiya, M., Hernandez Acosta, P., Garcia-Verdugo, J. M., Sunabori, T., Sakaguchi, M., Adachi, K., Kojima, T., Hirota, Y., Kawase, T. et al. (2006). Subventricular zone-derived neuroblasts migrate and differentiate into mature neurons in the post-stroke adult striatum. *J. Neurosci.* **26**, 6627-6636.